北京大學
PEKING UNIVERSITY

Using Fractal Theory to Study the Influence of Movable Oil on the Pore Structure of Different Types of Shale

A Case Study of the Fengcheng Formation Shale in Well MY1 of Mahu Sag, Junggar Basin, China

Hong Zhang

Institute of Energy, Peking University

May 14, 2024

Contents

Background

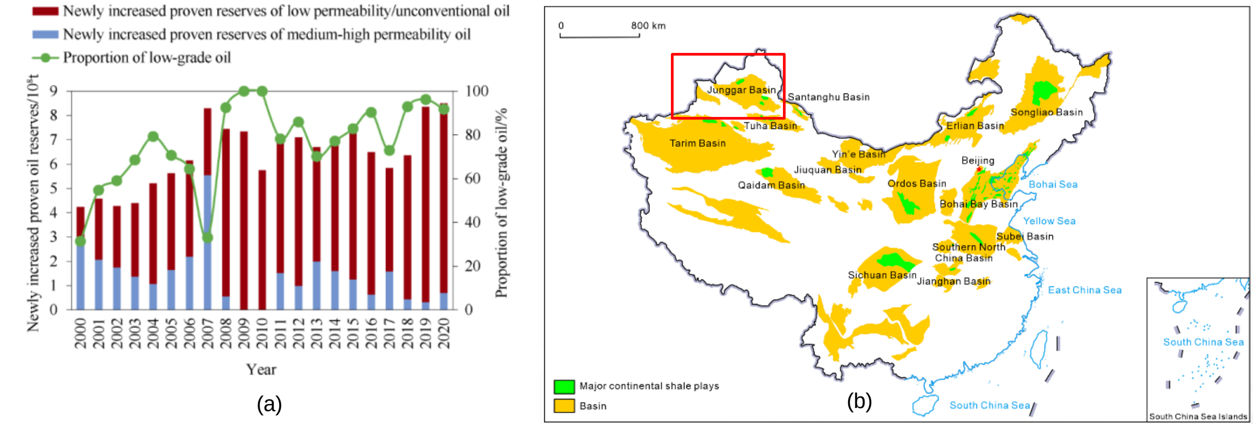

Figure 1. (a) Composition of newly increased proven oil reserves of CNPC; (b) distribution of continental shale oil plays in China(Modified from Pang et al., 2023)

Geological Setting

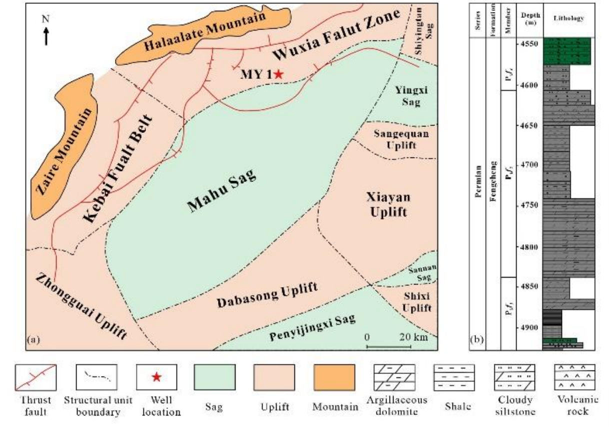

Figure 2. (a) Structural setting of the Mahu Sag, Junggar Basin and sampling location of Well MY1; (b) columnar graph of lithology of Well MY1

- In the northwestern region of the Junggar Basin
- Semi-deep to deep alkaline lake sedimentation
- The samples were mainly distributed in the lower member (P_1f_1) and the middle member (P_1f_2) of the formation

Methods

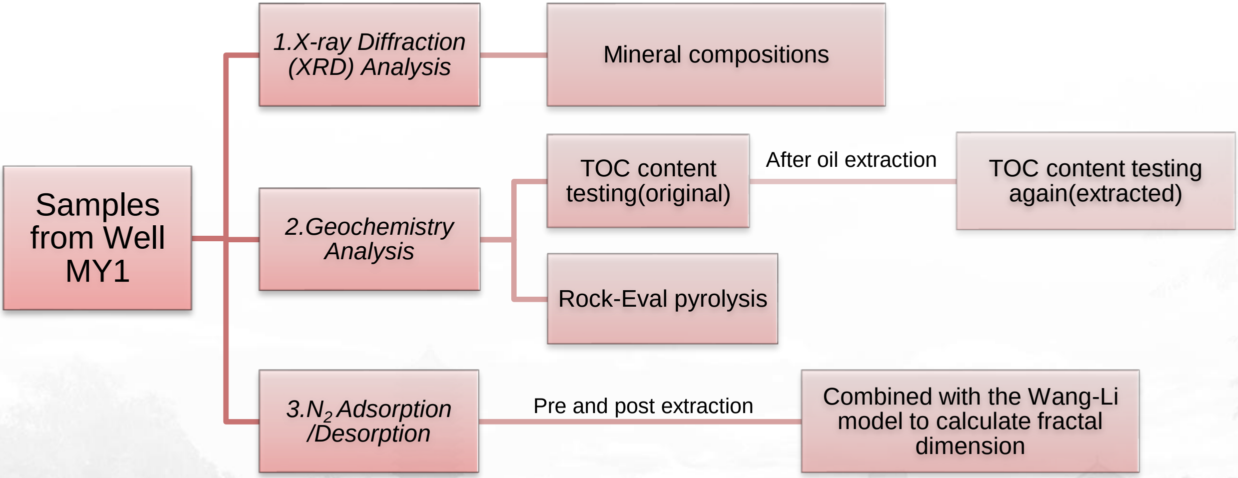

Samples from Well MY1
1.X-ray Diffraction (XRD) Analysis
Mineral compositions
2.Geochemistry Analysis
TOC content testing(original)
After oil extraction
TOC content testing again(extracted)
Rock-Eval pyrolysis
3.N_2 Adsorption /Desorption
Pre and post extraction
Combined with the Wang-Li model to calculate fractal dimension

Mineral Compositions

Table 1. Sample number, depth, lithology and mineralogical parameters obtained by XRD analysis.

Sample Number	Depth (m)	Lithology (wt.%)	Qtz + Fsp (wt.%)	Total Carb (wt.%)	Total Clay (wt.%)	Pyrite (wt.%)	Type
1	4716.34	Argillaceous silty dolomite	29.7	62.5	4.2	3.6	I
2	4738.73	Dolomitic mudstone	45.1	40.6	9.5	4.8	III
3	4740.43	Silty argillaceous dolomite	50.9	39.2	6.4	3.5	II
4	4744.9	Silty dolomitic mudstone	61.6	33.1	2.5	2.7	II
5	4751.36	Dolomitic mudstone	38	50.5	9.9	1.7	I
6	4759.42	Argillaceous dolomite	41.5	52.5	4.4	1.5	I
7	4766.56	mudstone	54.7	38.7	3.7	3.0	II
8	4773.99	Silty argillaceous fine sandstone	66.6	22.6	3.2	7.6	II
9	4790.94	Dolomite argillaceous fine sandstone	66	25.6	2.9	4.4	II
10	4799.67	Dolomite silty mudstone	39.9	56	3.1	1.1	I
11	4800.45	Dolomitic mudstone	46.7	49.8	2.3	1.2	I
12	4800.98	Silty mudstone	57	33.1	4.3	5.5	II
13	4802.2	Argillaceous dolomitic fine sandstone	36.1	44	13.7	3.8	III
14	4804.95	Dolomitic fine sandstone	69.9	15.5	6.6	6.8	II
15	4816.79	Calcareous mudstone	40.8	55.3	1.2	2.7	I
16	4830.31	Fine sandy dolomite	56.4	32.6	5.7	3.8	II
17	4835.28	Silty dolomite	37.9	50.4	7.4	4.3	I
18	4850.43	Silty argillaceous fine sandstone	61.3	16.8	9.2	7.6	II
19	4851.11	Dolomitic silty mudstone	61.6	16.3	9	7.2	II

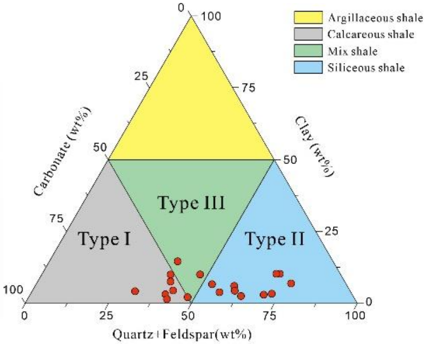

Figure 3. Triangular plot of shale mineral composition

- Type I: calcareous shale (carbonate mineral content >50%)
- Type II: siliceous shale (felsic mineral content > 50%)

北京大学 PEKING UNIVERSITY

Geochemical Properties

Table 2. TOC content of samples before and oil extraction.

TOC variation	Type Ⅰ		Type Ⅱ	
	Range(%)	Average(%)	Range(%)	Average(%)
Before extraction	0.54-1.04	0.78	0.46-1.42	0.90
After extraction	0.38-0.94	0.58	0.27-0.85	0.55

- The extraction process has a certain impact on samples of different types.
- Siliceous shale have a greater amount of movable oil compared to calcareous shale.

N_2 Adsorption and Desorption Isotherms

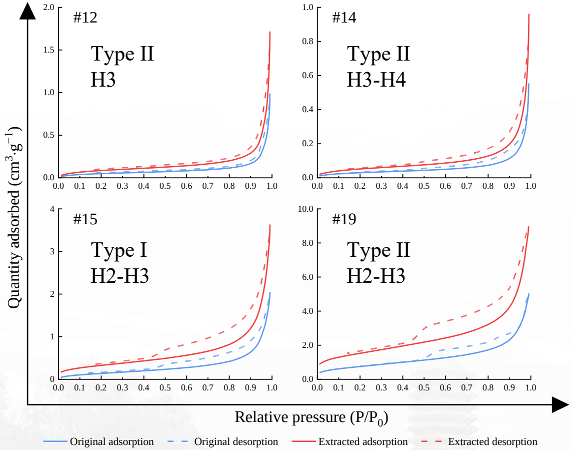

Figure 4. Isothermal adsorption-desorption curves of typical samples before and after extraction.

- For Type I (calcareous shale): like sample #15, ink-bottle-shaped pores
- For Type II (siliceous shale), the hysteresis loops can be divided:
  - ✓ slit-shaped pores with parallel plates(sample #12)
  - ✓ slit-like pores that are open all around(sample #14)
  - ✓ ink-bottle-shaped pores(sample #19)

北京大学 PEKING UNIVERSITY

Fractal Analysis of Gas Adsorption

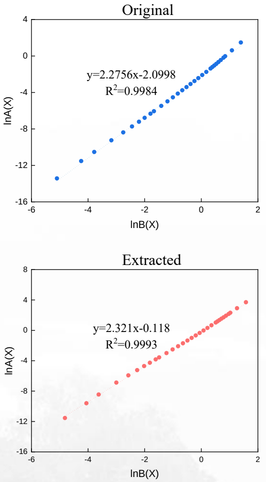

Figure 5. The Wang–Li fractal analysis of sample #8 (adsorption branch).

Let

$$A(X) = \frac{-\int_{N(X)}^{N_{max}} \ln(X)\, dN(X)}{r^2(X)}, \qquad B(X) = \frac{[N_{max} - N(X)]^{1/3}}{r(X)} \tag{1}$$

Then

$$lnA(X) = constant + D \times lnB(X) \tag{2}$$

Table 3. Calculating the fractal dimension of shale samples using Wang–Li fractal theory.

Type I				Type II			
Samples	$D_{original}$	$D_{extracted}$	ΔD	Samples	$D_{original}$	$D_{extracted}$	ΔD
1	2.2298	2.2306	0.0008	3	2.2425	2.2406	−0.0019
5	2.2499	2.2508	0.0009	4	2.3157	2.3093	−0.0064
6	2.2099	2.2131	0.0032	7	2.226	2.2256	−0.0004
10	2.2257	2.2261	0.0004	8	2.2756	2.321	0.0454
11	2.1921	2.1911	−0.001	9	2.2282	2.234	0.0058
15	2.2347	2.2307	−0.004	12	2.4024	2.4054	0.003
17	2.2022	2.2004	−0.0018	14	2.2335	2.2329	−0.0006
				16	2.1759	2.1765	0.0006
				18	2.3096	2.3124	0.0028
				19	2.3367	2.3373	0.0006
Average	2.2206	2.2204	−0.0002	Average	2.2746	2.2795	0.0049

Fractal Analysis of Gas Adsorption

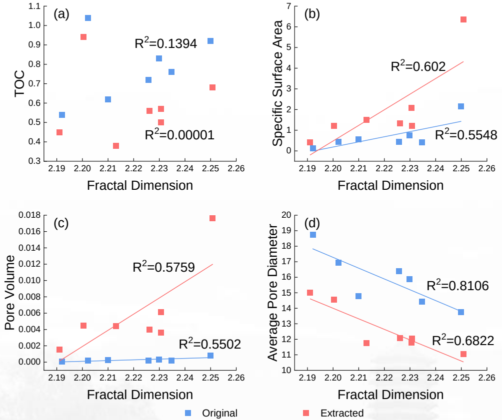

Figure 6. Relationships between fractal dimension and TOC (a), specific surface area (b), pore volume (c) and average pore diameter (d) of Type I samples.

- The fractal dimension appeared to be predominantly influenced by the pore structure, including parameters such as pore-specific surface area, pore volume, and average pore diameter (Figure 6 b–d).

Fractal Analysis of Gas Adsorption

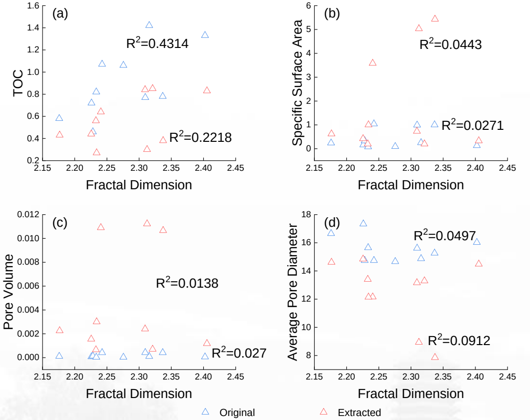

Figure 7. Relationships between fractal dimension and TOC (a), specific surface area (b), pore volume (c) and average pore diameter (d) of Type II samples.

- For the changes in fractal dimension of siliceous shales before and after oil extraction, we believe that they are the result of the combined effects of TOC and pore structure. Of the two factors, TOC may play a more important role.

Conclusions

(1) Organic solvent extraction significantly reduced TOC content, with a greater impact on siliceous shale than calcareous shale, indicating higher movable oil content in the former.

(2) Calcareous shale (Type I) exhibited prevalent H2–H3 type hysteresis loops, indicating a uniform pore structure, while siliceous shale (Type II) showed diverse loop types, highlighting its complex pore structure.

(3) Oil extraction increased specific surface area and pore volume in both shale types, particularly in quartz-feldspathic mineral-dominated shale, due to the release of hydrocarbon-occupied pore space.

(4) Fractal dimension changes in carbonate mineral-dominated shale were influenced by pore structure, not TOC, while in quartz-feldspathic mineral-dominated shale, changes were not clearly correlated with TOC or pore structure, suggesting a combined effect, possibly with TOC playing a significant role.

Thank You!